

Seismic Hazard Assessment for Faro, YK

Final Report:
May 2004

Prepared for:
DELOITTE & TOUCHE INC.
Interim Receiver of Anvil Range Mining Corporation
Suite 1900, 79 Wellington Street West
Toronto, ON M5K 1B9 Canada

Prepared by:
Gail M. Atkinson, Ph.D.
Engineering Seismologist
280 McLean Ave.
Arnprior, ON K7S 3T2 Canada

**Deloitte
& Touche**

Seismic Hazard Assessment for Faro, YK

Final Report:
May 2004

Table of Contents

Introduction and Problem Description	Page 2
Seismic Hazard Analysis for Faro	Page 3
<i>Methodology</i>	Page 3
<i>Input Parameters</i>	Page 5
<i>Results</i>	Page 8
Conclusions	Page 9
References	Page 9

List of Figures

Figure 1	GSC calculations for PGA at Faro
Figure 2	Seismicity of Faro region
Figure 3	Magnitude recurrence relation for Tintina zone
Figure 4	Median results for Faro for NEHRP C
Figure 5	Results at Faro for NEHRP C
Figure 6	Soil amplification factors to apply to go from NEHRP C to NEHRP D
Figure 7	Detailed hazard results at Faro
Figure 8	Detailed view of PGA versus probability at Faro
Figure 9	Spectra for $p=0.0001$ per annum at Faro

List of Appendices

Appendix A	Seismic Hazard Model Values for Faro from the Geological Survey of Canada
Appendix B	Input Parameters for Faro Seismic Hazard Analysis
Appendix C	Geologic Review by H. R. Smith (2004)

Seismic Hazard Assessment for Faro, YK

Introduction and Problem Description

A limited site-specific seismic hazard analysis has been performed for Faro, Yukon (62.2N 133.2W) that addresses the issues raised regarding an apparent linear alignment of seismicity in the region along the Tintina Trench fault system (Cassidy et al., 2003; Hyndman et al., 2003) and its implications for the Faro site, including consideration of uncertainty. The rationale for the hazard assessment is as follows.

There have been several seismic hazard studies for the Anvil Range Mining Complex at Faro, YK, as summarized in the SRK report of Oct. 2003 prepared for Deloitte and Touche Inc. The studies date back to 1981. For a variety of reasons, ranging from outdated reference material for the older studies, to incomplete or inappropriate seismicity catalogues and ground motion relations for some of the newer studies, none of these studies provides an adequate portrayal of the seismic hazards at Faro. In addition, there has been significant new geologic and seismicity data gathered in recent years, as summarized by Hyndman et al. (2003) and Cassidy et al. (2003).

The most credible seismicity assessment at Faro to date is that provided by the national seismic hazard maps, as determined by the Geological Survey of Canada (Adams and Halchuck, 2003). The GSC calculation, which is based on a broad regional model for the Yukon seismicity, is given in Appendix A. Figure 1 shows a plot of the probability of exceedence versus peak ground acceleration (PGA) at Faro according to the GSC model, where the GSC curve has been extrapolated out to a probability of 10^{-4} per annum (p.a.) in order to provide a very rough indication of low probability motions.

A significant shortcoming of the GSC model when applied to Faro is that it is based on very broad regional source zones, which may not reflect local tectonic details, and may thus not be appropriate for use at low probability levels or for site-specific analysis. Figure 2 shows all seismicity in the Faro region, along with the two alternative GSC source zone models that are used in the national hazard maps (the maps use the most conservative of the results from the two models). The regions surrounding the GSC sources used for Faro are much more active than Faro seismically, but will contribute little to hazard at Faro due to the large distances of these outside hazard sources from Faro (>200 km). From Figure 2, it appears that there is a linear band of seismicity running southeast to northwest through the Faro site, which is not well described by the broad regional source zones. This linear band of seismicity has also been noted by Cassidy et al. (2003). The linear band is significant for two reasons: (i) it may indicate active faulting along the Tintina Trench fault system with which it is coincident; and (ii) it appears that the Tintina Trench is more active than the surrounding areas, all of which were lumped together in the GSC source zone for the southern Yukon. If the Tintina system is more active than the surrounding areas, then the GSC calculations will underestimate hazard for sites near the Tintina Trench.

A review of the regional bedrock geology and faults by Smith (2004), attached as Appendix C to this report, suggests that the linear trend of seismicity seen on Figure 2 is spatially coincident with similar linears in regional faults which are part of the Tintina Trench fault system (see Smith's Figure 2). Thus it is reasonable to suppose that there may be linear faults that trend to the northwest through Faro that are acting to localize seismicity. It should be noted that the earthquakes are probably happening at depths of about 10 km, and may not be related to the specific fault structures mapped on the surface; however the coincidence of fault trends with seismicity trends suggests the likelihood that similar structures exist at seismogenic depths. This is confirmed by the appended Smith (2004) report, which cites evidence that the Tintina Trench is a major regional geologic feature of wide crustal extent and reduced crustal strength. The recent studies reported by Hydman et al. (2003) also suggest that the Tintina Trench plays an important role in regional tectonics. A study by Doig (1998) suggests that there may have been two shaking events that disturbed sediments in Fisheye Lake, along the Tintina Trench near Faro, within the last 1000 years. Consequently, a seismic hazard analysis at Faro should consider the possibility of a seismic source zone that includes the northwest trending fault structures and seismicity surrounding the Tintina Trench.

Seismic Hazard Analysis for Faro

Methodology

I have conducted a site specific seismic hazard analysis for Faro using the FRISK88 software (Risk Engineering, Inc.). This is the same probabilistic seismic hazard software used by the Geological Survey of Canada in the national seismic hazard maps. This section provides an overview of the methodology. The method, as it applies to the national seismic hazard maps, is summarized by Adams and Atkinson (2003).

Seismic hazard analyses in Canada are based on probabilistic concepts which allow incorporation of both geologic interpretations of seismic potential and statistical data regarding the locations and sizes of past earthquakes. The Cornell-McGuire method (Cornell, 1968; McGuire, 1976, 1977, 1995; Risk Engineering, 1988) has proven particularly well-suited to calculate expected ground motions for a wide range of seismic hazard environments, offering flexibility in the consideration of spatial and temporal characteristics of regional earthquake occurrence, and the basic physics of the earthquake process.

The spatial distribution of earthquakes is described by defining seismic source zones (faults or areas) on the basis of seismotectonic interpretations; the earthquake potential of these zones is generally assumed to be uniform. The frequency of earthquake occurrence within each source zone is described by a magnitude recurrence relationship, truncated at an upper magnitude bound, M_x . Earthquake ground motion relations provide the link between the occurrence of earthquakes of various magnitudes and the resulting ground motion levels at any site of interest. The probability of exceeding a specified level of ground motion at a site can then be calculated by integrating hazard contributions over all magnitudes and distances, including all source zones. To obtain ground motion

levels or spectra for a desired probability, calculations are repeated for a number of ground motion values, for all desired ground motion parameters.

The Cornell-McGuire framework has been well-accepted in all parts of North America. In Canada, it forms the basis for the seismic hazard maps in the National Building Code of Canada (NBCC, 1985 and beyond), and is the usual basis for seismic hazard evaluations of all important engineered structures.

It has long been recognized that seismic hazard analyses are subject to greater uncertainties than those associated with most environmental loads, but their full implications for design have only recently been addressed in standard practice. Two types of uncertainty exist: (i) random uncertainty (aleatory uncertainty) due to the physical variability of earthquakes processes (eg. the stochastic nature of the location of future events and of source and path processes); and (ii) professional uncertainty (epistemic uncertainty) due to incomplete understanding of the physics governing earthquake occurrence and ground motion generation (eg. selection and characterization of source zones, relations giving median ground motion levels, etc.).

The first type of uncertainty is readily incorporated within the Cornell-McGuire analysis framework, and is included in a standard 'best-estimate' seismic hazard result. The second type of uncertainty implies a spread of possible results about those that might be considered a best-estimate. It has been noted that this type of uncertainty can cause differences in results, among different investigators, of factors of much more than two. Uncertainties of this magnitude have major implications in the design of engineered facilities. In the past, they have often been ignored, leading to a very incomplete picture of the true hazard. Alternatively, they have been examined through sensitivity analyses, which can lead to ambiguities in interpretation, since the spread in results will depend on the likelihood of the tested scenarios.

Recent developments in seismic hazard analysis have focused on a more rigorous treatment of uncertainty in the input parameters (type (ii) uncertainties). The FRISK88 program used in this study (Risk Engineering, 1988) utilizes a logic tree approach to represent each input parameter by a simple probability distribution. For example, instead of inputting a single value for the maximum magnitude of each source zone, the user specifies several possible values and their associated probabilities. Uncertainties in the following parameters are treated in this fashion: seismic source models, configuration of specific sources, recurrence parameters, maximum magnitudes, and ground motion relations. In this study, uncertainty in the seismic source models is of particular importance, given the seismicity along the Tintina Trench.

The FRISK88 program performs multiple hazard calculations, to provide the result and associated weight (probability) for every possible combination of input parameters. In this report, these results (typically there are hundreds to thousands for each site and ground motion parameter) are summarized by providing mean ground motions, and ground motions for the 84th, 50th (median) and 16th percentiles (eg. corresponding roughly to plus or minus one standard deviation for a normal distribution). The mean

hazard curve is our best estimate of the true hazard given the current uncertainties; it is the best estimate. However, the median curve (for which half of the estimates lie above, and half lie below) is sometimes preferred because it is less influenced by uncertainties, and in particular is less influenced by extreme scenarios included in the hazard curves. The national seismic hazard maps are based on the median curve (Adams and Atkinson, 2003). The hazard fractiles can be interpreted as confidence limits: for example, we are 84% confident that the true seismic hazard curve lies below the 84th percentile.

To utilize the capabilities of FRISK88, we require a description of seismic hazard parameters and their uncertainties. This includes the delineation of the region into alternative source zone models, representing alternative tectonic interpretations of the seismicity, with estimates of the likelihood that each zonation model is the 'true' model. Within each source model, alternative geometric configurations (and associated weights) may be specified for each individual source, if desired. For this study, several alternative models for the Tintina Trench seismicity were considered.

For each source zone of each model, magnitude recurrence parameters and their uncertainty are modeled by alternative ν , β pairs (eg. rate and slope of the Gutenberg - Richter recurrence relation), with associated weights. Three pairs were used for each source zone. Maximum magnitudes for each source zone were also specified by three alternative values. For each ground motion parameter, three alternative ground motion relations were defined; parameters included the 5% damped pseudo-acceleration (average horizontal component), for frequencies of 0.5 to 10 Hz, plus peak ground acceleration. The alternatives for each input parameter were selected to represent our current 'best' estimate (given a weight of 40% to 60%), a 'worst-case' scenario (with weight of 10% to 20%), and an 'optimistic' scenario (weight of 10% to 30%).

Input Parameters

To explore the main uncertainties in seismic hazard assessment at Faro, while keeping the scope of the study limited, I have used the GSC national hazard model (as summarized in Adams and Atkinson, 2003) as a starting point, then added in consideration of the uncertainties that are specific to the Faro site. In essence, I use the GSC regional model, but include alternative definitions for the seismogenic source zone in which Faro is located. Appendix B lists the model parameters employed in the analysis by FRISK88.

The most important new input parameters concern the Faro zone. Figure 2 shows the defined source zone to encompass the linear trend of seismicity that follows the Tintina Trench. Figure 3 shows the best-estimate magnitude recurrence relation for this source zone, along with an upper and lower bound estimate that reflects uncertainty. The magnitude scale used in the catalogue is local magnitude, M_L , which is believed to be approximately equal to moment magnitude for events in this region (Cassidy et al., 2003). The annual rates shown for each magnitude level on Figure 3 were calculated based on the time periods for which each magnitude level was completely reported within the Geological Survey of Canada seismicity database. These time periods were determined by evaluation of the catalogue data over time, and by considering instrument deployment

patterns, as summarized by Cassidy et al., 2003. The completeness criteria are somewhat optimistic for the lowest magnitudes, which may not be completely reported. This can be seen by inspection of the magnitude recurrence relation; the reported rates are falling below the Gutenberg Richter relation at the lowest magnitudes. The adopted time windows for preparation of the magnitude recurrence relation of Figure 3 are:

- $M > 3$ since 1980
- $M > 5$ since 1950
- $M > 6$ since 1920

The observed seismicity rates can be checked against geologic strain rates. Cassidy et al. (2003) and Hyndman et al. (2003) report that there has been between 450 and 1000 km of right-lateral displacement along the Tintina Trench since mid to late-Cretaceous time (about 65 million years ago), which translates to a slip rate of about 8 mm/year. They also cite GPS data that indicates current strain of no more than about 5 mm/year along this system. Other geologic evidence (cited by Smith, 2004) suggests that the strain rate at present might be closer to 1 mm/year. Thus the geologic strain rate is somewhere in the range from 1 to 10 mm/year.

The current seismicity rates can be used to calculate a geologic strain rate, assuming that the relationship between earthquake magnitude (moment magnitude, M) and average fault displacement (AD, in m) is as given by the empirical relations of Wells and Coppersmith (1994) for strike-slip earthquakes:

$$\text{Log AD} = -6.32 + 0.90 M$$

For the magnitude recurrence relations shown on Figure 3, the corresponding strain rates can be obtained by summing up the displacements obtained by the above equations over all magnitudes from 5.5 to the maximum magnitude. The obtained strain rates are in the range from 1 to 10 mm/year, depending on the case selected (best-estimate, worst case or optimistic case) and the assumed maximum magnitude. Overall, a strain rate near 4 mm/year is supported by the seismicity, which agrees with the geologic rates. Thus we can be fairly confident that the magnitude recurrence relations shown represent the long-term seismicity on the Tintina system, as well as current seismicity rates.

The maximum magnitude of the recurrence relation is the value at which the relation is truncated: the probability of events larger than M_x is assumed to be zero. A range of M_x values for Tintina was considered, from moment $M = 6.7$ (lower value) to $M = 7.8$ (upper value), with the best estimate being assigned $M = 7.2$. The relative weights assigned to these values are 0.68 (best estimate), 0.16 and 0.16. This follows the conventions used by the GSC in similar tectonic zones. It suggests that very large events (such as those seen on the Denali Fault System) may be possible on the Tintina, but it is most likely that the maximum magnitudes are more moderate (low 7s).

In implementing the Tintina model in the hazard calculations, I consider several alternatives, with given weights (summing to 1) reflecting their relative credibility, as follows:

- 0.33 weight to the GSC Southern Yukon model of regional seismicity
- 0.34 weight to the Tintina zone model of Figure 3, treated as an area source
- 0.33 weight to the Tintina Trench being treated as a fault source (eg. a line source rather than an area source), with weights within this scenario given as follows:
 - 0.11 weight to a fault near Faro dipping 45 degrees east
 - 0.11 weight to a vertical fault near Faro
 - 0.11 weight to a fault near Faro dipping 45 degrees west.

The line source for the Tintina fault source scenario is a line that bisects the area source shown on Figure 2 (passing through the point 62N 133W, and within about 20 km of Faro). The line source is assumed to have the same seismicity level as used for the area source (but note that the sources are alternative scenarios, so that the total seismicity is preserved in each case). The range of dips for the Tintina fault represents our lack of knowledge concerning how this fault behaves. Fault ruptures along the line are assumed to follow the Wells and Coppersmith (1994) empirical relation between rupture length and magnitude.

All other input parameters for the calculations, and their uncertainties, are as given in the GSC model. These include the seismicity parameters for the surrounding source zones, which include the Mackenzie Mountains and the Denali Fault zones (of the GSC H model); all other source zones are too distant to exert any influence on the hazard calculations. The ground motion relations are also taken directly from the GSC model; these are the crustal relations developed by Boore et al. (1997), modified to match observed attenuation rates in western Canada as described by Atkinson (1995). An upper and a lower alternative for the ground motion relations is also adopted directly from the GSC model.

The calculations are performed for a reference site condition of NEHRP C. NEHRP C sites are very dense soil and soft rock, with shear-wave velocity (averaged over the top 30m) of 360 to 760 m/sec, or blow counts of greater than 50. However the Faro site is believed to be NEHRP D based on blow count data. NEHRP D sites are stiff soil sites with blow counts of 15 to 50, and shear-wave velocities in the range from 180 to 360 m/sec. Thus final results need to be amplified from C to D, using the soil amplification factors provided in the national seismic hazard maps and building code (see Adams and Halchuck, 2003). These factors are shown below; they represent soil amplification for NEHRP D sites relative to the NEHRP C sites for which the hazard calculations were made, where the amplification factor depends on the amplitude level of the spectrum (SA, given in units of g) for the NEHRP C sites, in order to represent nonlinearity of response at high amplitude.

For frequencies ≥ 5 Hz:

	For SA(5Hz) $\leq 0.25g$	0.50	0.75	1.00	1.25
D amplification =	1.3	1.2	1.1	1.1	1.0

For frequencies ≤ 1 Hz

	For SA(1Hz) $\leq 0.25g$	0.50	0.75	1.00	1.25
D amplification =	1.4	1.3	1.2	1.1	1.1

These factors are shown in Figure 6. The high-frequency factors are applied to $f \geq 5$ Hz and PGA (peak ground acceleration), while the low-frequency factors are applied to $f \leq 1$ Hz. Linear interpolation between the two factors is used for intermediate frequencies.

Results

The analysis results include a family of ground motion curves, reflecting uncertainty in the results according to uncertainty in the input parameters. For example, we can be 84% confident that the true ground motions for the 10^{-4} per annum (p.a.) probability level lie below the plotted 84th percentile results, based on current knowledge. The results are given for the random horizontal component response spectra, for 5% damping, in cm/s^2 .

Results are shown in a number of formats. Figure 4 is an overview of median results for a range of probability, for NEHRP C conditions (the reference condition, for which all hazard calculations were performed). The median results are the 50th percentile: half of the results are lower than this, while half of the results are higher. Figure 5 is detailed view of the results for NEHRP C, showing various confidence levels. Figure 5 also shows the expected ground motions for scenario events that could be selected to match the design event, according to the ground motion relations of Boore et al. (1997). This indicates that an earthquake of approximately **M**7 at 10 to 20 km would be a good match for most of the 10^{-4} spectrum, with the distance depending on the desired level of confidence.

Figure 7 shows the corresponding spectra amplified to NEHRP D, using the factors shown on Figure 6. On Figures 4, 5 and 7, the PGA is plotted at a frequency of 50 Hz for reference. Figure 8 is a detailed view of the PGA hazard curve for NEHRP D conditions.

The choice of design event for time history selection (for use in time history analyses) depends on the desired level of confidence. It is my understanding based on discussions with the project team that a high level of confidence, corresponding to motions near the mean of the 0.0001 p.a. spectrum, is desired. On this basis, a search of existing time histories from past earthquakes was made, using the COSMOS database. The search looked for records of western North American events of **M** 6.7 to 7.3 at distances from 10 to 30 km from the fault, having PGA in the range from 0.3 g (median level for 0.0001 p.a.) to 0.5g (mean level for 0.0001 p.a.), and recorded on rock or firm ground conditions. Rock-like conditions were sought, as it is understood that the effects of local foundation soils will be explicitly included in the response analysis of the facilities. Six three-

component records were identified, with four being from the Loma Prieta earthquake (**M** 7.0) and two being from the Northridge earthquake (**M**6.7). Inspection of the response spectra of these records indicates that three are suitable as design time histories for Faro, based on general similarity with the Faro 0.0001 p.a. spectrum, in the median-to-mean range. Figure 9 plots the horizontal components (two per record) for the three selected time histories, in comparison to the 0.0001 p.a. Faro spectra for NEHRP C conditions, along with the average spectrum of the six selected horizontal components. As with all natural records, there is much frequency-to-frequency variability of the response spectral ordinates. Overall, the selected time histories average between the median and the mean over most frequencies. High-frequency spectra and PGA generally lie between the median and mean. At frequencies of 2 to 5 Hz the records tend to lie near the mean, with individual records often lying above the mean in some frequency ranges. At frequencies less than 1 Hz the records are near the median, with only 1 record component (from Gilroy3) lying at or above the mean. Thus to ensure that the mean spectrum is satisfied in an overall sense, the analyses should be conducted to ensure satisfactory performance with all six time histories. The time history files for these records are attached as an electronic supplement.

Conclusions

A seismic hazard analysis has been performed for the Faro, Yukon site, considering regional seismicity and regional geologic features, including the Tintina Trench. For an annual probability of exceedence of 0.0001, corresponding to a 10,000 year return period ground motion, the mean value of peak ground acceleration (PGA) at Faro is 546 cm/s² for NEHRP D soil conditions. NEHRP D is the soil condition that is believed to apply to the Faro site. The mean value of PGA includes the effects of uncertainty on amplitude, and is our best estimate of the expected value. A less conservative estimate of the PGA is the median value, which corresponds to the value that we are 50% confident will not be exceeded for the given probability level. The median PGA on NEHRP D for Faro, at the 0.0001 per annum probability, is 343 cm/s². These ground motions correspond to an earthquake of approximately **M**7, at a distance of 10 to 20 km from the Faro site.

References

- Adams, J. and G. Atkinson (2003). Development of seismic hazard maps for the 2003 National Building Code of Canada. *Can. J. Civ. Eng.*, **30**, 255-271.
- Adams, J., and Halchuk, S. 2003. Fourth generation seismic hazard maps of Canada: Values for over 650 Canadian localities intended for the 2005 National Building Code of Canada. Geological Survey of Canada Open File 4459 150 pp.
- Atkinson, G. (1995). Attenuation and source parameters of earthquakes in the Cascadia region. *Bull. Seism. Soc. Am.*, **85**, 1327-1342.
- Boore, D. W. Joyner and T. Fumal (1997). Equations for estimating horizontal response spectra and peak acceleration from western North American earthquakes: A summary of recent work. *Seism. Res. L.*, **68**, 128-153.
- Cassidy, J., G. Rogers and J. Ristau (2003). Seismicity in the vicinity of the SNORCLE corridors of the northern Canadian Cordillera. *Can. J. Earth Sci.*, Special SNORCLE review volume, submitted.

- Cornell, C. (1968). Engineering seismic risk analysis. *Bull Seism. Soc. Am.*, **58**, 1583-1606.
- Doig, R. (1998). Paleoseismological evidence from lake sediments for recent movement on the Denali and other Faults, Yukon Territory, Canada. *Tectonophysics*, **296**, 363-370.
- Hyndman, R., P. Fluck, S. Mazzotti, T. Lewis, J. Ristau and L. Leonard (2003). Constraints on current tectonics of the northern Canadian Cordillera. *Can. J. Earth. Sci.*, special SNORKLE volume, submitted.
- McGuire, R. (1976). FORTRAN computer program for seismic risk analysis. U.S. Geol. Surv. Open-file Rpt. 76-67.
- McGuire, R. (1977). Seismic design spectra and mapping procedures using hazard analysis based directly on oscillator response. *Intl. J. Earthq. Eng. Struct. Dyn.*, **5**, 211-234.
- McGuire, R. (1995). Probabilistic seismic hazard analysis and design earthquakes: Closing the loop. *Bull. Seism. Soc. Am.*, **85**, 1275-1284.
- Risk Engineering (1988). FRISK88 User's Manual.
- Wells, D. and K. Coppersmith (1994). New empirical relationships among magnitude, rupture length, rupture width, rupture area, and surface displacement. *Bull. Seism. Soc. Am.*, **84**, 974-1002.

Figures

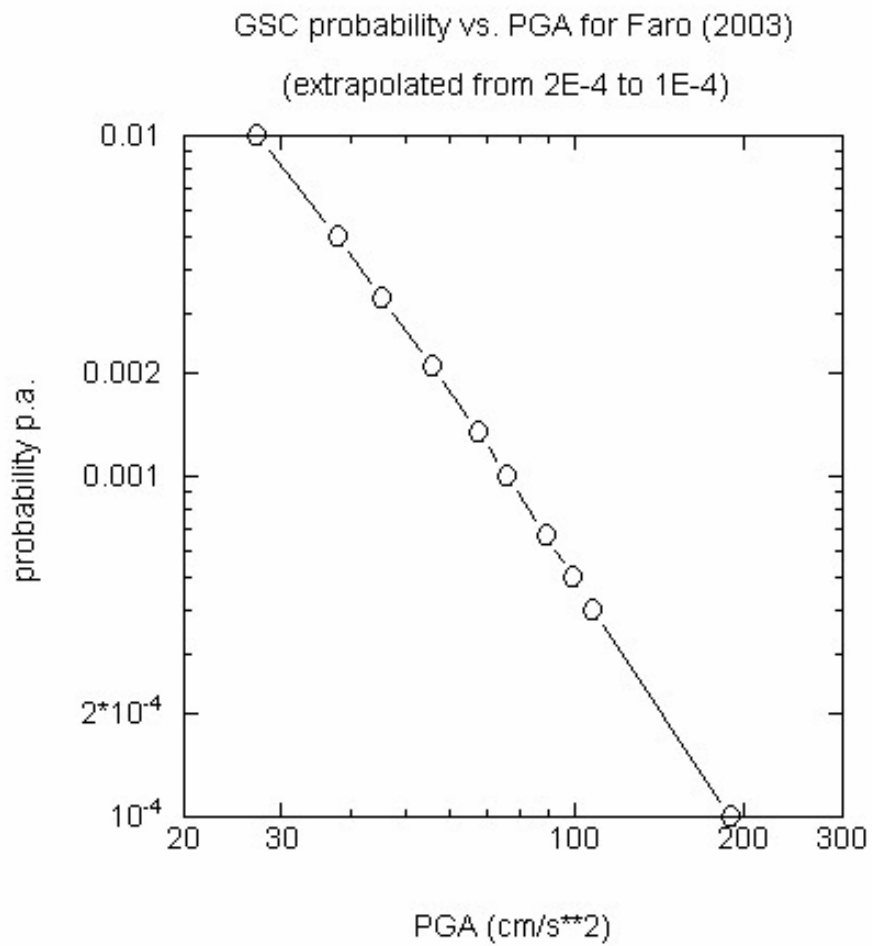


Figure 1 – GSC calculations for PGA at Faro (firm ground (NEHRP C) site conditions).

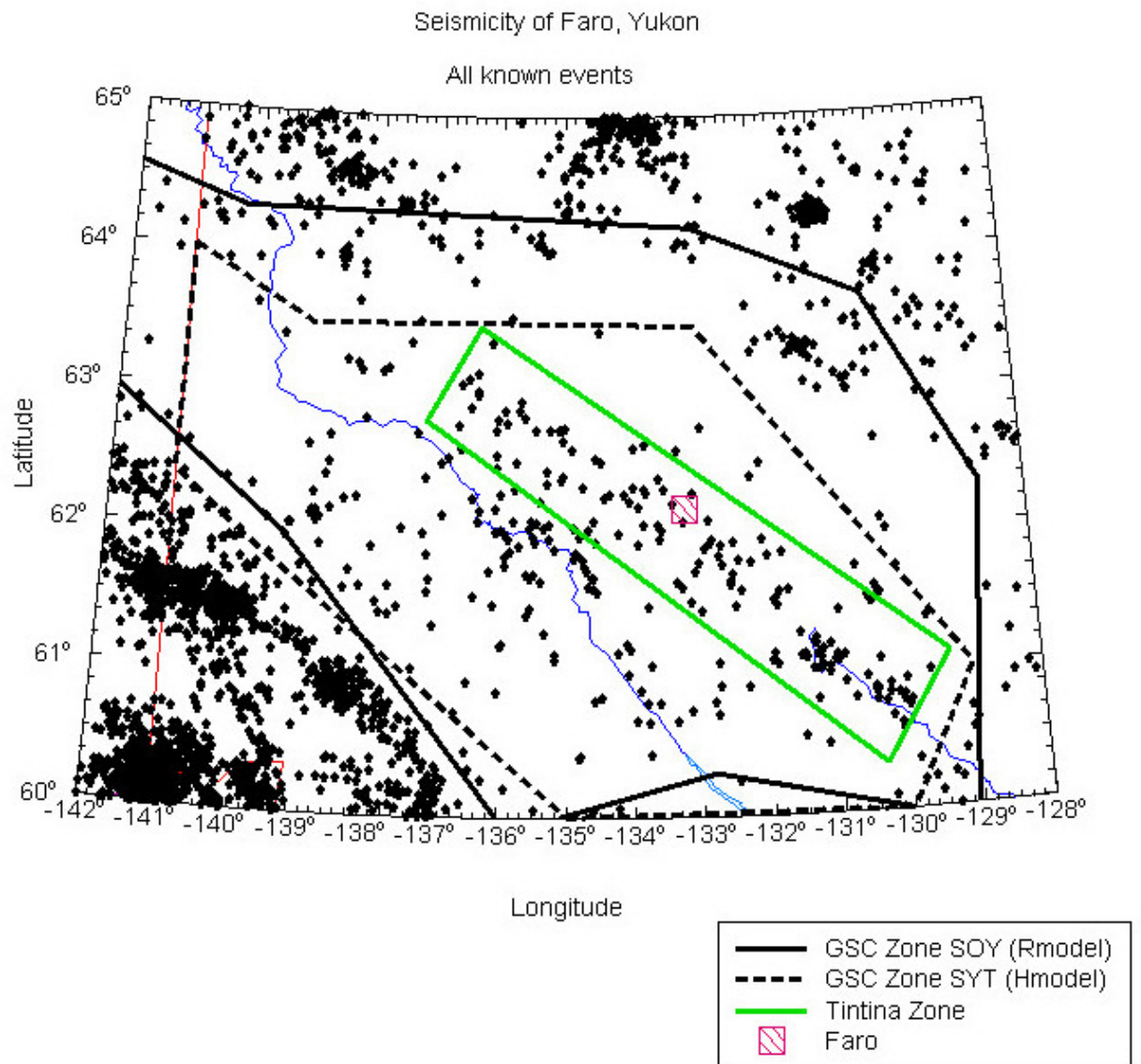


Figure 2 – Seismicity of Faro region – all known events. Green box outlines apparent linear trend of seismicity along Tintina Trench

Magnitude Recurrence - Tintina Zone

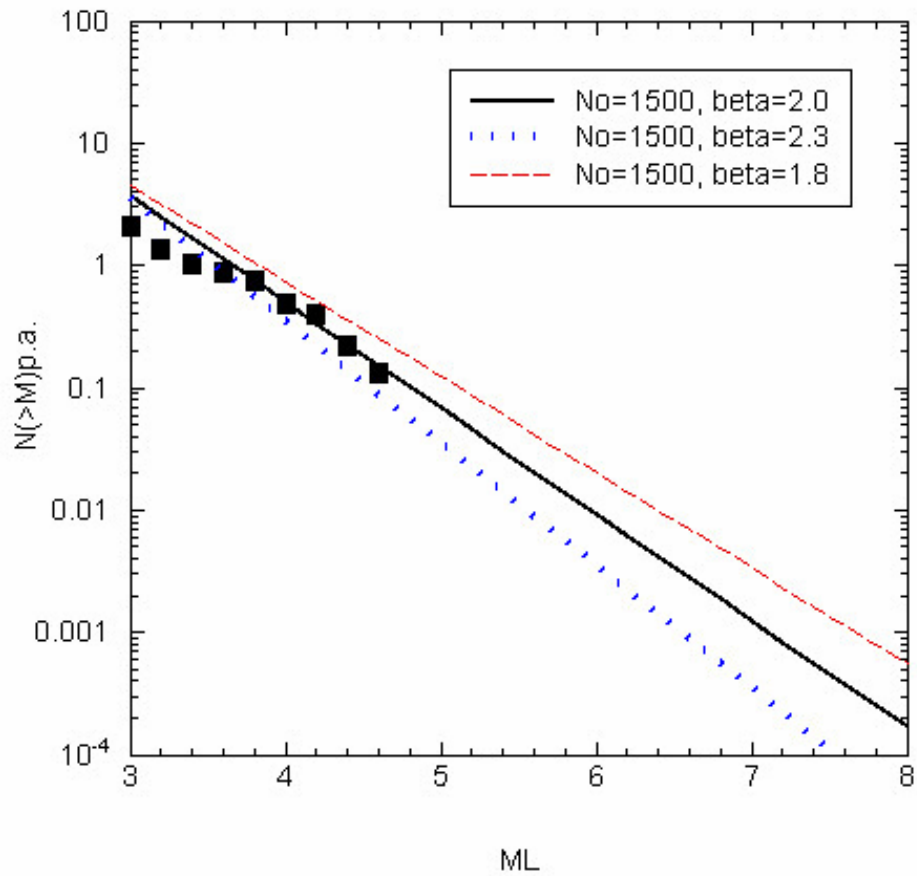


Figure 3 – Magnitude recurrence relation for Tintina zone. Symbols are observed rates of activity (not complete at $M < 3.5$). Lines show best estimate model for hazard analysis (black solid line) along with assumed uncertainty.

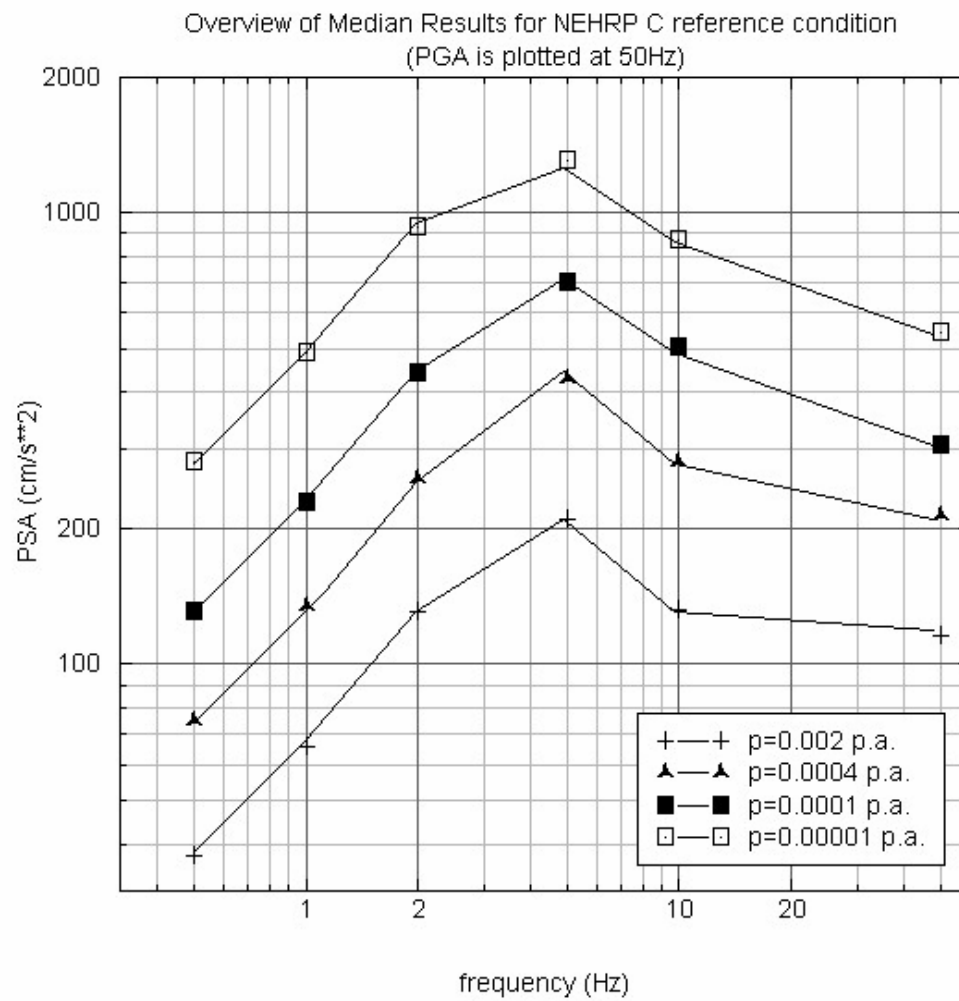


Figure 4 – Median results for Faro for NEHRP C (reference site condition for calculations), for various probability levels. PGA is plotted at 50 Hz.

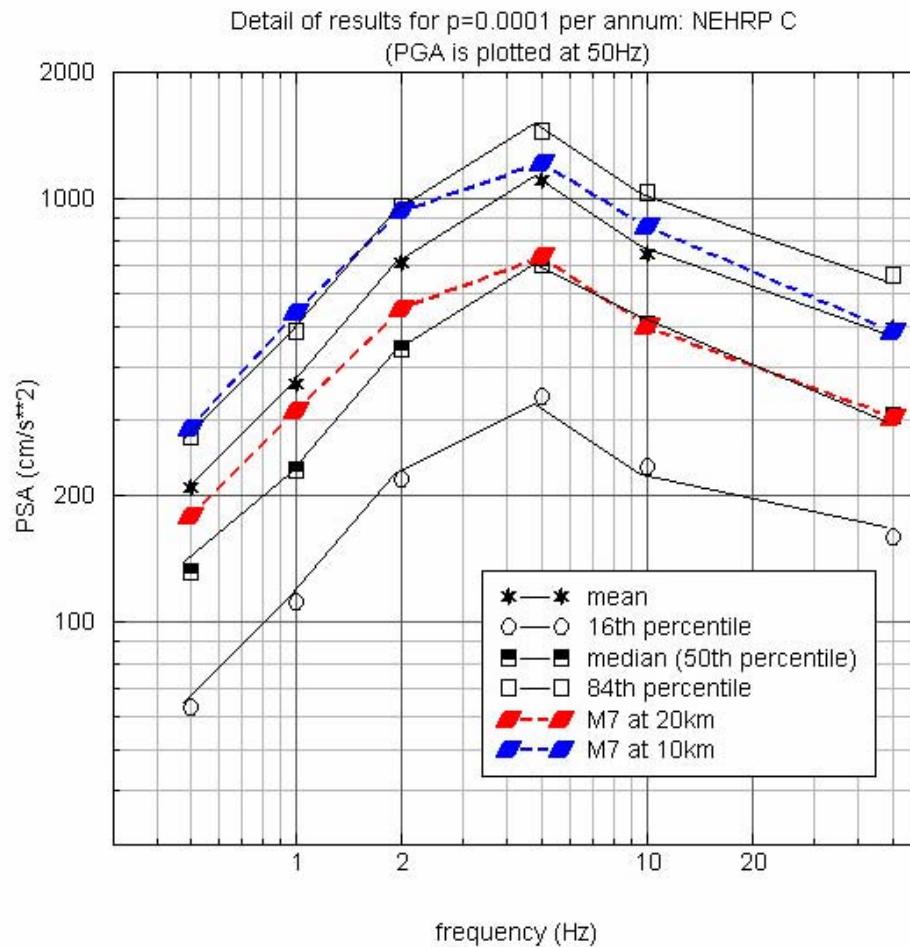


Figure 5 – Results at Faro for NEHRP C, for annual probability of 10^{-4} per annum. Curves include uncertainty; thus we are 84% certain the true result lies below the 84th percentile. PGA is plotted at 50 Hz. Coloured lines show the amplitudes for potential design or scenario events to match the target spectrum: a M7 at 10 to 20 km.

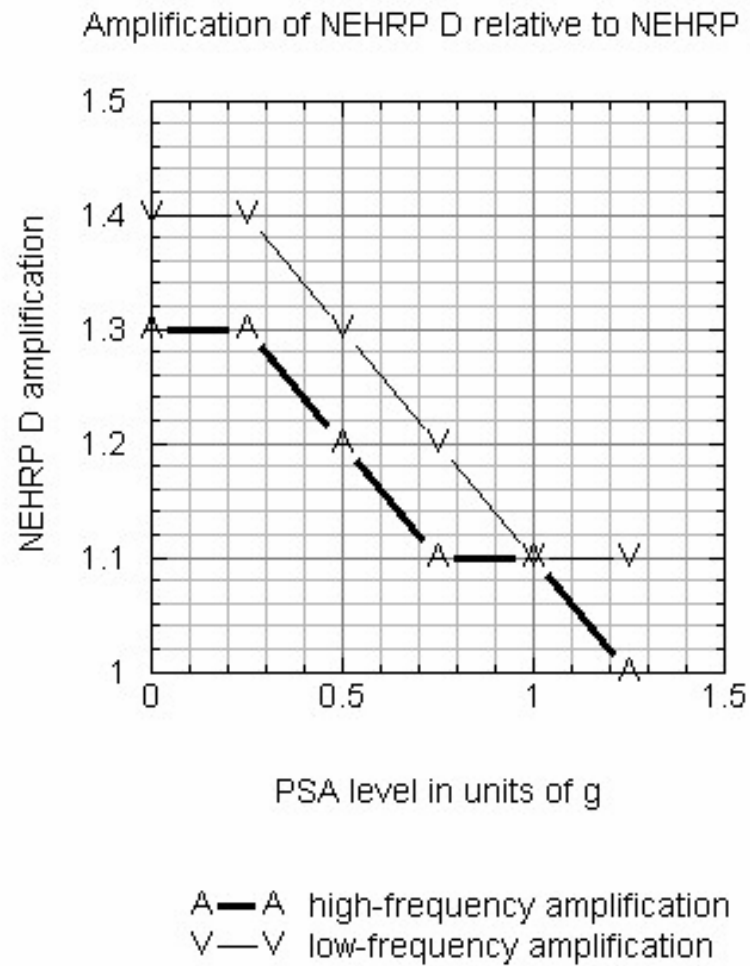


Figure 6 – Soil amplification factors to apply to go from NEHRP C to NEHRP D conditions. A values apply to high frequencies (>5 Hz) and PGA, while V values apply to lower frequencies (0.5 to 1 Hz).

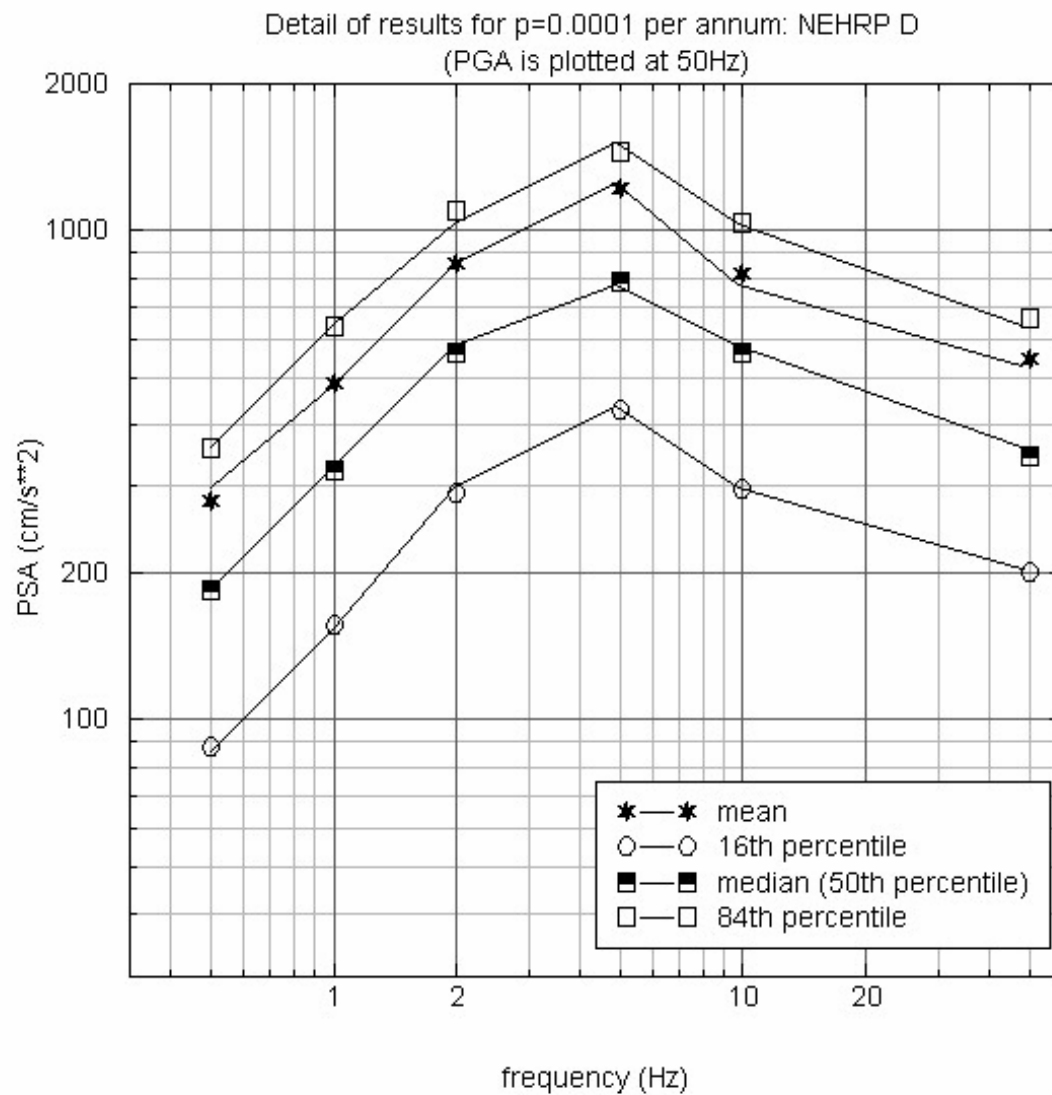


Figure 7 – Detailed hazard results at Faro, for $p=0.0001$ per annum, for NEHRP D conditions. PGA is plotted at 50 Hz.

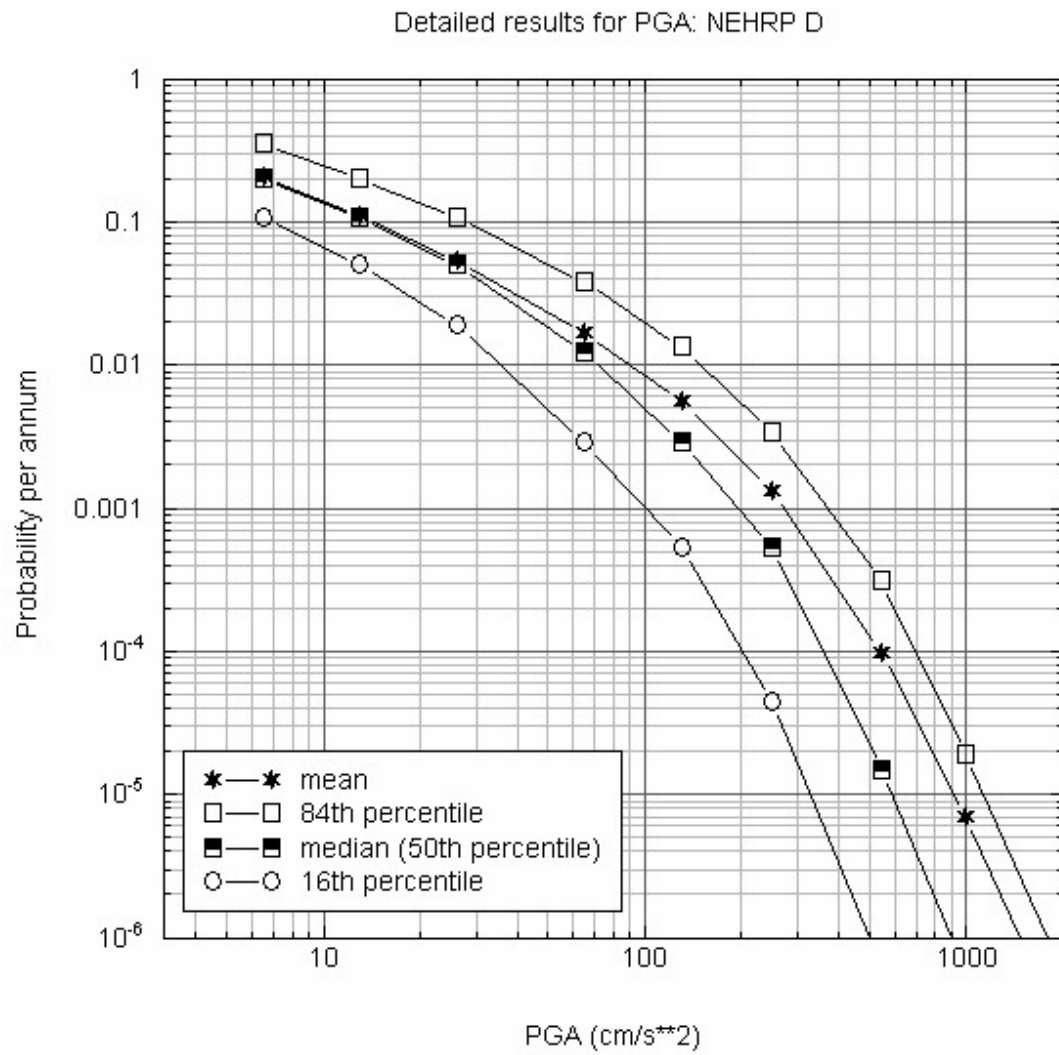


Figure 8 – Detailed view of PGA versus probability at Faro, for NEHRP D conditions.

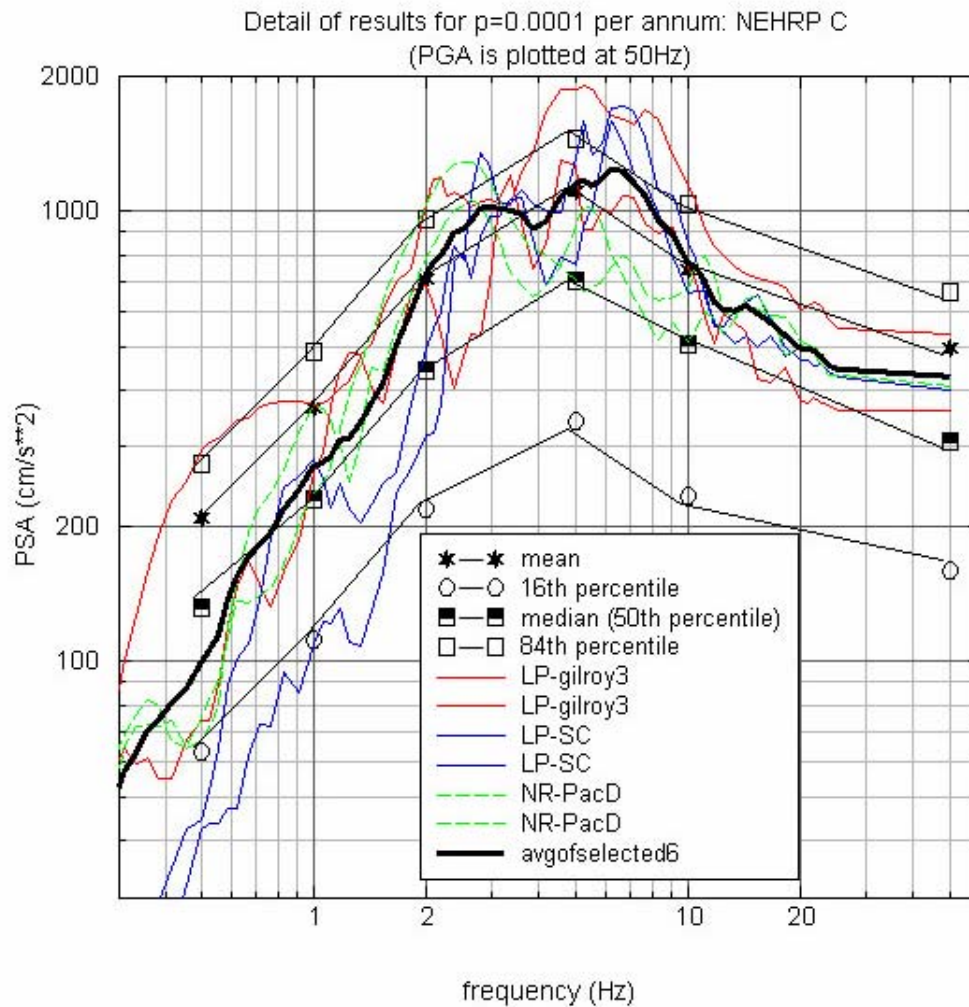


Figure 9 – Spectra for $p=0.0001$ per annum at Faro, for NEHRP C conditions, in comparison to the spectra of selected time histories. Records denoted LP are from the Loma Prieta earthquake (Gilroy3 and Lick Observatory); records denoted NR are from the Northridge earthquake (downstream record of Pacoima Dam).

Appendix A
Seismic Hazard Model Values for Faro from the Geological Survey
of Canada

Appendix A: Seismic Hazard Model Values for Faro from the Geological Survey of Canada, as received by email from Stephen Halchuck, GSC.

Note: complete hazard maps are available from Adams and Halchuck, 2003, from www.seismo.nrcan.gc.ca

Subj:Re: hazard computation for Faro, YK
Date:07/11/2003 10:18:55 Eastern Standard Time
From:halchuk@seismo.nrcan.gc.ca
To:Gmatkinson@aol.com
CC:adams@seismo.nrcan.gc.ca
Sent from the Internet (Details)

Hi Gail

Below find the values for Faro, YK.....

I've provided values from 0.01 to 0.000404 (2%/50 years). At the moment, it is not our intention to provide lower probability values.

Here are some of the words we've been giving to clients who request the 1/10000 values:

1/10,000 return periods are normally only required for special facilities such as nuclear power plants or dams which have a large consequence if they were to fail. These 1/10,000 return periods are beyond the scope of the National Building Code of Canada. Extrapolation of the hazard model to lower probability results is mathematically possible, but represents an unreliable extrapolation of the seismic source zones used to develop the seismic hazard model.

Also of note is the fact that the models were developed for the National Building Code of Canada, which is intended for standard structures. These may not be the most appropriate models for critical structures. If your project requires it (because of the consequences of failure), a site-specific hazard assessment developed by consulting engineers may be required. For screening purposes (to decide if a full assessment is needed), you could seek advice as to the design standards being applied by (the former) Ontario Hydro or Hydro-Quebec to similar facilities.

Having said that, we will try to give you some guidance by providing you with the 10%/50 year (1/475 year or 0.0021 per annum probability) values from the proposed 2005 National Building Code. You can then plot

these two sets of values on a log-log scale and extrapolate them out to the 1/10000 year return period, with the understanding that we cannot vouch for the validity of these extrapolated values at your particular site.

on a log-log scale these values are almost linear, so the extrapolation, should the client choose to use it, won't be unreasonable.

Sa(0.2) for Faro, YK 5hz
62.200 -133.200 0.010000 46.5
62.200 -133.200 0.005000 65.9
62.200 -133.200 0.003330 80.2
62.200 -133.200 0.002100 99.8
62.200 -133.200 0.001330 123.0
62.200 -133.200 0.001000 140.1
62.200 -133.200 0.000667 167.6
62.200 -133.200 0.000500 189.9
62.200 -133.200 0.000404 208.1
Sa(0.5) for Faro, YK 2hz
62.200 -133.200 0.010000 31.9
62.200 -133.200 0.005000 43.6
62.200 -133.200 0.003330 52.1
62.200 -133.200 0.002100 63.7
62.200 -133.200 0.001330 77.4
62.200 -133.200 0.001000 87.2
62.200 -133.200 0.000667 103.3
62.200 -133.200 0.000500 116.3
62.200 -133.200 0.000404 127.0
Sa(1.0) for Faro, YK 1hz
62.200 -133.200 0.010000 18.4
62.200 -133.200 0.005000 24.6
62.200 -133.200 0.003330 29.1
62.200 -133.200 0.002100 34.9
62.200 -133.200 0.001330 41.8
62.200 -133.200 0.001000 46.7
62.200 -133.200 0.000667 54.6
62.200 -133.200 0.000500 61.0
62.200 -133.200 0.000404 66.2
Sa(2.0) for Faro, YK 0.5hz
62.200 -133.200 0.010000 11.7
62.200 -133.200 0.005000 15.4
62.200 -133.200 0.003330 18.1
62.200 -133.200 0.002100 21.5
62.200 -133.200 0.001330 25.5
62.200 -133.200 0.001000 28.3

62.200 -133.200 0.000667 32.8
62.200 -133.200 0.000500 36.4
62.200 -133.200 0.000404 39.3
PGA for Faro, YK
62.200 -133.200 0.010000 27.0
62.200 -133.200 0.005000 37.8
62.200 -133.200 0.003330 45.4
62.200 -133.200 0.002100 55.5
62.200 -133.200 0.001330 67.3
62.200 -133.200 0.001000 75.6
62.200 -133.200 0.000667 88.7
62.200 -133.200 0.000500 99.3
62.200 -133.200 0.000404 107.5

cheers
Stephen

Appendix B

Input Parameters for Faro Seismic Hazard Analysis

Appendix B: Input parameters for Faro seismic hazard analysis (example given for f=1 Hz)

```

*****
*****      PROGRAM FRISK88 FOR      *****
*****      SEISMIC HAZARD CALCULATION *****
*****      RISK ENGINEERING, INC.   *****
*****      GOLDEN, CO USA          *****
*****

-133.2, 62.2      Full Faro Model 2003/12/17  1 Hz PSA  NEHRP C conditions

INPUT AND INTEGRATION CONTROL VARIABLES:
      NATTS NSTEP DZ      ECIN AMSTEP NRL  JPRINT
        3    20  5.00    5.0  0.05    1    1

HAZARDS WILL BE CALCULATED FOR THE FOLLOWING AMPLITUDES
      5.00    10.00    20.00    50.00    100.00    200.00    500.00    1000.00    2000.00

SITE COORDINATES:  -133.20    62.20

WEIGHTS OF ATTENUATION FUNCTIONS:      0.30 0.40 0.30

TYPES OF SOURCES TO BE CONSIDERED:
      B: BOTH FAULTS AND AREAS WILL BE CONSIDERED

TRUN.
NO ATTEN type  C1   C2   C3   C4   C5   C6  RZERO R0  JC SIGMA CODE PAR ID
1      F   2.82  0.45 -0.01-.00097-0.80 0.31 2.90  0.0  2 0.62 0 0.0 2
      A           2.82  0.45 -0.01-0.00097 -0.80 0.31 0.00  0.0  2
0.62  0  0.000

2      F   2.52  0.45 -0.01-.00097-0.80 0.31 2.90  0.0  2 0.62 0 0.0 2
      A           2.52  0.45 -0.01-0.00097 -0.80 0.31 0.00  0.0  2
0.62  0  0.000

3      F   2.22  0.45 -0.01-.00097-0.80 0.31 2.90  0.0  2 0.62 0 0.0 2
      A           2.22  0.45 -0.01-0.00097 -0.80 0.31 0.00  0.0  2
0.62  0  0.000

NUMBER OF GLOBAL ALTERNATIVES, PROBABILITY OF EACH:
      1 1.0000

*****
*****
GLOBAL ALTERNATIVE 1: H model sources DENH and MCK, plus Faro alternatives SYT,
FaroArea, and 3 FaroFa
*****
*****

NSETS NPAIRS NMAX NDEPTH MAXSRC MAXPTS
      3      3      3      1      7      20

WEIGHTS FOR PARAMETER ASSUMPTIONS
      MAXIMUM MAGNITUDE WEIGHTS      0.68 0.16 0.16
      NU-BETA PAIR WEIGHTS           0.68 0.16 0.16
      DEPTHS                          1.00

DEPENDENCE OF PARAMETERS:
      MAX MAGNITUDES:      PERFECT DEPENDENCE
      NU BETA PAIRS:      PERFECT DEPENDENCE
      DEPTH ASSUMPTIONS:  PERFECT DEPENDENCE
      ATTENUATION ASSUMPTIONS: PERFECT DEPENDENCE

*****
*****

```

```

SOURCE SET 1, DENALI FAULT
.....

SOURCE NUMBER 1A SOURCE NAME: DENH SOURCE TYPE: area
WEIGHT: 1.0000
DEPTH VALUES: 2.90
COORDINATES OF: area DENH ( TOTAL NUMBER OF POINTS= 11)
(-145.000 63.700) (-140.000 62.000) (-135.500 59.800) (-135.700 59.000)
(-136.000 59.300) (-136.500 59.600) (-138.000 59.330) (-138.000 59.670)
(-139.000 60.500) (-141.000 61.000) (-145.000 63.000)

SEISMICITY ASSUMPTIONS USED:
MIN. MAGNITUDE= 4.75 MAX. MAGNITUDES= 7.50 7.00 8.00
MAGNITUDE DISTRIBUTION: EXPONENTIAL
NU BETA VALUES: 0.37100 1.8540 0.29300 1.9472 0.48600 1.7607

*****
*****

SOURCE SET 2, MCKENZIE MOUNTAINS
.....

SOURCE NUMBER 2A SOURCE NAME: MCK SOURCE TYPE: area
WEIGHT: 1.0000
DEPTH VALUES: 2.90
COORDINATES OF: area MCK ( TOTAL NUMBER OF POINTS= 11)
(-136.000 65.700) (-134.000 65.700) (-125.000 65.700) (-123.000 64.000)
(-123.000 60.000) (-126.300 59.000) (-129.000 61.000) (-133.000 63.500)
(-137.500 63.500) (-137.500 65.000) (-139.000 65.700)

SEISMICITY ASSUMPTIONS USED:
MIN. MAGNITUDE= 4.75 MAX. MAGNITUDES= 7.20 6.90 7.50
MAGNITUDE DISTRIBUTION: EXPONENTIAL
NU BETA VALUES: 1.01100 2.2054 0.90000 2.2762 1.21500 2.1347

*****
*****

SOURCE SET 3, SOUTHERN YUKON TERRITORY/ FARO
.....

SOURCE NUMBER 3A SOURCE NAME: syt SOURCE TYPE: area
WEIGHT: 0.3300
DEPTH VALUES: 2.90
COORDINATES OF: area syt ( TOTAL NUMBER OF POINTS= 9)
(-141.000 64.000) (-139.000 63.500) (-133.000 63.500) (-129.000 61.000)
(-130.000 60.000) (-135.000 60.000) (-135.500 59.800) (-140.000 62.000)
(-141.000 62.400)

SEISMICITY ASSUMPTIONS USED:
MIN. MAGNITUDE= 4.75 MAX. MAGNITUDES= 7.00 6.70 7.30
MAGNITUDE DISTRIBUTION: EXPONENTIAL
NU BETA VALUES: 0.05580 1.9283 0.02460 2.2452 0.11300 1.6114
.....

SOURCE NUMBER 3B SOURCE NAME: faroarea SOURCE TYPE: area
WEIGHT: 0.3400
DEPTH VALUES: 2.90
COORDINATES OF: area faroarea ( TOTAL NUMBER OF POINTS= 4)
(-136.330 63.500) (-129.330 61.000) (-130.330 60.330) (-137.170 62.830)

SEISMICITY ASSUMPTIONS USED:
MIN. MAGNITUDE= 4.75 MAX. MAGNITUDES= 7.20 6.70 7.80
MAGNITUDE DISTRIBUTION: EXPONENTIAL
NU BETA VALUES: 0.11200 2.0000 0.06300 2.3000 0.19400 1.8000
.....

SOURCE NUMBER 3C SOURCE NAME: farofault1 SOURCE TYPE: fault
WEIGHT: 0.1100

```

```

    DIP1  DIP2   Z1    Z2    Z3
  90.00  90.00   1.00  10.00 20.00

  RUPTURE LENGTH EQUATION PARAMETERS:
        AL      BL      SIGL
    -3.2200  0.6900  0.2200

  COORDINATES OF: fault farofault1                ( TOTAL NUMBER OF POINTS= 2)
  (-130.000  60.830) (-136.000  63.000)

  SEISMICITY ASSUMPTIONS USED:
    MIN. MAGNITUDE= 4.75    MAX. MAGNITUDES= 7.20 6.70 7.80
    MAGNITUDE DISTRIBUTION:      EXPONENTIAL
    NU BETA VALUES: 0.11200 2.0000 0.06300 2.3000 0.19400 1.8000
  .....

  SOURCE NUMBER    3D  SOURCE NAME: farofault2          SOURCE TYPE: fault
  WEIGHT:    0.1100
        DIP1  DIP2   Z1    Z2    Z3
    45.00  45.00   1.00  10.00 20.00

  RUPTURE LENGTH EQUATION PARAMETERS:
        AL      BL      SIGL
    -3.2200  0.6900  0.2200

  COORDINATES OF: fault farofault2                ( TOTAL NUMBER OF POINTS= 2)
  (-130.000  60.830) (-136.000  63.000)

  SEISMICITY ASSUMPTIONS USED:
    MIN. MAGNITUDE= 4.75    MAX. MAGNITUDES= 7.20 6.70 7.80
    MAGNITUDE DISTRIBUTION:      EXPONENTIAL
    NU BETA VALUES: 0.11200 2.0000 0.06300 2.3000 0.19400 1.8000
  .....

  SOURCE NUMBER    3E  SOURCE NAME: farofault3          SOURCE TYPE: fault
  WEIGHT:    0.1100
        DIP1  DIP2   Z1    Z2    Z3
    135.00 135.00   1.00  10.00 20.00

  RUPTURE LENGTH EQUATION PARAMETERS:
        AL      BL      SIGL
    -3.2200  0.6900  0.2200

  COORDINATES OF: fault farofault3                ( TOTAL NUMBER OF POINTS= 2)
  (-130.000  60.830) (-136.000  63.000)

  SEISMICITY ASSUMPTIONS USED:
    MIN. MAGNITUDE= 4.75    MAX. MAGNITUDES= 7.20 6.70 7.80
    MAGNITUDE DISTRIBUTION:      EXPONENTIAL
    NU BETA VALUES: 0.11200 2.0000 0.06300 2.3000 0.19400 1.8000
  *****
                                  END OF INPUT
  *****

```

Appendix C – Geologic Review by R. Smith (2004)

Appendix C
Geologic Review by H. R. Smith (2004)

WATER MANAGEMENT CONSULTANTS

May 19, 2004

130-10691 SHELLBRIDGE WAY
RICHMOND, B.C. V6X 2W8,
CANADA

TELEPHONE: (604) 273 6299
TELEFAX: (604) 270 3644

Steffen Robertson & Kirsten (Canada) Inc.
Suite 800, 1066 West Hastings Street
Vancouver, B.C., Canada, V6E 3X2

Attention: Cam Scott, P.Eng.
Principal, Geotechnical Engineering

Re: Tectonic setting
Faro, Yukon

Dear Sir:

This letter has been prepared at your request to provide a preliminary understanding of the tectonic setting of the Faro region. The Faro site is located in central Yukon (see Figure 1). The community was established in support of the operating mine. The community of Faro is located within the Tintina Trench and the mine site is located in the sub parallel valley of Rose Creek, Northeast of the Tintina Trench. The mine is no longer operating and mine closure activities are under way. For structures that will remain in perpetuity, design parameters for long term performance are required. For high risk structures, the potential for seismic loading due to rare large events needs to be considered.

Following is a brief discussion to provide a background for definition of design earthquake parameters for the closed facilities at the Faro mine site. The purpose of this letter is to provide background information that can be used to complete an assessment of appropriate seismic design parameters. This letter has been prepared based on reading of technical papers and communication with individuals. A list of references is appended.

Yukon Geology

In Yukon, there are two main geological components separated primarily by the Tintina Fault. The northeasterly region is composed of a thick older sequence of sedimentary rocks that was deposited upon a stable geological basement. The region southwest of Tintina Fault is composed of a younger, complex mosaic of varying rock types that amalgamated and accreted to the stable sedimentary package.

The northeasterly rocks are old, mainly sedimentary and represent the ancient North American margin. Prior to 190 million years ago, the western edge of the ancient North American continent extended far out into the Pacific Ocean. This submerged continental shelf provided a stable continental platform upon which sediments, dominantly limestone

and sandstone accumulated. Shale, sandstone and chert accumulated in adjacent basins. Parts of a similar (or the same) assemblage can also be found west of the Tintina trench (Cassiar Platform).

The mosaic of accreted and amalgamated terranes to the southwest are different from each other and are separated by faults. Most of the terranes are different from rocks of the ancient North American continent and their place of origin is uncertain. Some terranes are similar to ancient North American, but cannot be absolutely correlated. Geological evidence further suggests that several of these terranes may have amalgamated with each other prior to their accretion to ancient North America.

The lithoprobe program (Clowes et al, 2003) identified westward dipping layers from outcrops in the Foreland Belt. Along Line 3 (through Ross River), the layering is visible between 5 and 12 seconds (15 to 36 km). The layering is disrupted at the Tintina fault zone. This implies that 1) ancient North American crust and lithosphere project westward beneath most of the Northern Cordillera, 2) the detachments that carry deformed rocks of the northern Canadian Cordillera are largely confined to the crust above the layering, and 3) rocks of most of the accreted terranes overlie this layer. Most of the accreted rocks thus appear to be thin (<10 km thick), far flung flakes.

Tintina Fault

The long linear depression that extends northwesterly across the Yukon from Watson Lake along to Ross River, Faro and Dawson, and then into Alaska is the Tintina Trench. It is the northern continuation of the Northern Rocky Mountain Trench in British Columbia. The Tintina trench is the physiographic expression of the Tintina Fault. Tectonic forces caused the block of rocks southwest of the fault to move northwestward towards Alaska along the North American block. The motion would have been accompanied by significant earthquake activity and probably caused significant reduction of rock strength. The loss of strength has probably caused the rocks to be less resistant which, with erosion, led to the formation of the trench. Most geological evidence suggests at least 450 km of right lateral displacement along the Tintina Fault although some estimate there has been as much as 1200 km of offset.

Volcanic rocks were deposited in the trench about 55 million years ago. This volcanic deposition probably coincided with periods of motion along the Tintina Fault. These rocks are mapped in the trench at Faro and are often related to extensional activity (normal faulting).

The lithoprobe transect, which crosses the Tintina trench at Ross River identifies the Tintina fault zone as a vertical zone of little reflectivity.

Geologic Mapping

Geologic mapping of rock types has progressed over a number of years, primarily by the Geological Survey of Canada. The Yukon Geological Survey has made available an assemblage of the information on the Internet. They caution that any map obtained from the Internet is not a legal document and is subject to revision. A map from this source is presented as Figure 2.

Southwest of the Tintina Fault near Faro, sedimentary rocks associated with continental shelf deposits appear to be present. They are present for about 100 km southwest of Faro, where they are truncated by the Semenoff Fault. Mapping by de Keijzer et al confirm that North American terrane continues west of Tintina Trench.

The local geology, has been described by Jennings and Jilson (1986) and by Pigage (1999). The rocks include metasedimentary and metavolcanic units (chert, basalt, ultramafics, shale, phyllite, greenstone and schist) and granite of the Anvil Batholith. As illustrated on Figure 2, there are many faults mapped locally and in the region.

A significant fault (Vangorda fault zone) subparallel to the Tintina trench is mapped between the Faro orebody and the Tintina Fault. Although the Vangorda Fault zone may be related to the Tintina Fault, it does not have the physiographic expression expected of an active fault (the fault is along the ridge between Rose Creek and the Tintina Trench)

No information was located on surface expression of the faults along Rose Creek or along Tintina Trench.

Stress Distribution

There has been a long and varied stress history at this site as terranes to the southwest have accreted to the continental margin. This includes a potential for strike slip and shortening as well as a period of extension.

Currently, there is strong seismicity at long distance to the southwest, with subduction under Alaska and transpressive right lateral motion on the Denali Fault. In addition, there is strong seismicity to the northeast in the MacKenzie and Richardson Mountains. The main MacKenzie seismicity is on low angle thrust faults to the west of the main mountain front. In their discussion of this activity, Hyndman et al (2003) conclude that a small part of the Pacific/North American motion may be transmitted across the northern Cordillera with little intervening deformation. This distribution of crustal strain requires a quasi rigid displacement of the Cordilleran upper crust over a decoupling level (weak hot lower crust) that rises to join the basal detachment of thrusting in the foreland. Hyndman et al (2003) provide interpretations of stress directions within the major seismic areas based on earthquake mechanism solutions. They propose that collision of the Yukatut block in south western Alaska is creating strain, some of which is being transferred across the whole Cordillera. This implies that the Tintina Fault area is subject to this compressive stress.

Recent Ground Movements

Others have noted that there is no evidence of recent displacements along the Tintina Fault. However, the level of effort to locate and document recent movement in the Tintina trench near Faro is orders of magnitude lower than in areas such as California.

Jackson (2003) noted that, while mapping surficial geology in the area, no features were observed that indicated offset of glacial deposits in the Tintina Trench.

Doig (1998) cored sediments from several lakes in the Yukon in an effort to define seismic events based on resuspension of lake sediments. He concluded from core

extracted from Fisheye Lake near Faro that there have been two shaking events of unknown age, but possibly spanning an interval of more than 1000 years. He also observed that there is a 3 m (southwest side up) northwest trending vertical fault scarp on the lake bottom.

Earthquake Locations

Mazzotti and Hyndman (2002) note that there is a slight concentration of earthquakes to about magnitude 4.5 that suggests some activity of the right-lateral Tintina strike-slip fault zone. Although the data would suggest little deformation is occurring, it also implies that a weak zone is present along the trench. Most of the earthquakes have been located to the west of the trench. This may either imply that faults to the west are the active faults or that a systematic error is present in the model used for calculating epicenters.

Calculations described by Hyndman et al indicate that the crustal thickness is typically 20 to 30 km, so that most earthquake activity might be generated in the upper 20 km. Earthquake activity may be limited to 10 km depth as accreted terranes are typically less than 10 km thick.

Summary

Over the past two decades, several reports have been prepared that assumed the Tintina Fault is not active (see Steffen Robertson and Kirsten, 2003). However, recent research and earthquake monitoring have provided sufficient evidence that published reports now indicate that the Tintina Fault is active. In addition, examination of lake sediment cores from a site near Faro indicate that two major shaking events have probably occurred over the past 1,000 years or more. This supports the conclusion that the Tintina Fault is active, with rare large events.

Yours truly,

H.R.(Rod) Smith, P. Eng.

References

- Clowes R.M. (2003) Precambrian crust and lithosphere beneath the northern Canadian Cordillera discovered by lithoprobe seismic reflection profiling. Geophysical Research abstracts, Vol 5.
- Doig R. (1998) Paleoseismic evidence for lake sediments for recent movement on the Denali and other faults, Yukon Territory, Canada. Tectonophysics 296
- Edwards B.R. and J.K. Russell (1999) Northern Cordilleran volcanic province: A northern Basin and Range? Geology vol 27 no.3.
- Edwards B.R. and J.K. Russell (2000) Distribution, nature and origin of Neogene-Quaternary magmatism in the northern Cordilleran volcanic province, Canada. GSA Bulletin August 2000.
- de Keijzer M., P.F. Williams and R.L. Brown. (1999) Kilometre-scale folding in the Teslin zone, northern Canadian Cordillera, and its tectonic implications for the accretion of the Yukon-Tanana terrane to North America. Canadian Journal of Earth Science Volume 36
- Duk-Rodkin A. (2003) personal communication
- Frederikson A.W., M.G. Bostock, J.C. VanDecar and J.F. Cassidy (1998) Seismic structure of the upper mantle beneath the northern Canadian Cordillera from teleseismic travel-time inversion. Tectonophysics 294
- Hart C. (2002) The Geological Framework of the Yukon Territory.
<http://www.geology.gov.yk.ca/publications/summaries/framework.html>
- Hyndman R.D., P. Fluck, S. Mazzotti, T. Lewis, J. Ristau and L. Leonard, (2003). Constraints on Current Tectonics of the Northern Canadian Cordillera; Submitted for publication to Canadian Journal of Earth Sciences.
- Jackson L. (2003) personal communication
- Jennings D.S. and G.A. Jilson (1986) Geology and Sulfide deposits of Anvil Range, Yukon Territory. Mineral deposits of Northern Cordillera, J.A. Morin (ed) CIMM Special Volume 37.
- Lowe C., R.B. Horner, J.K. Mortensen, S.T. Johnston and C.F. Roots (1994) Canadian Journal of Earth Sciences Vol 31.
- Lowe C. and J.F. Cassidy (1995) Geophysical evidence for crustal thickness variations between the Denali and Tintina Fault Systems in west-central Yukon. Tectonics vol 14 no.4.
- Mazzotti S. and R. D. Hyndman (2002) Yakutat collision and strain transfer across the northern Canadian Cordillera. Geology; vol 30; no. 6.

Mazzotti S. (2003) personal communication

Pigage L.C. (1998) Preliminary Geology of Rose Mountain, Anvil District, central Yukon (105K/05). Yukon Exploration and Geology 1998, C. F. Roots and D. S. Emond (eds)

Pigage L. (2003) personal communication

Steffen Robertson and Kirsten (Canada) Inc. (2003) Information related to the Seismicity of the Anvil Range Mining Complex. A report prepared for Deloitte & Touche Inc.

Figure 1 - Site Plan

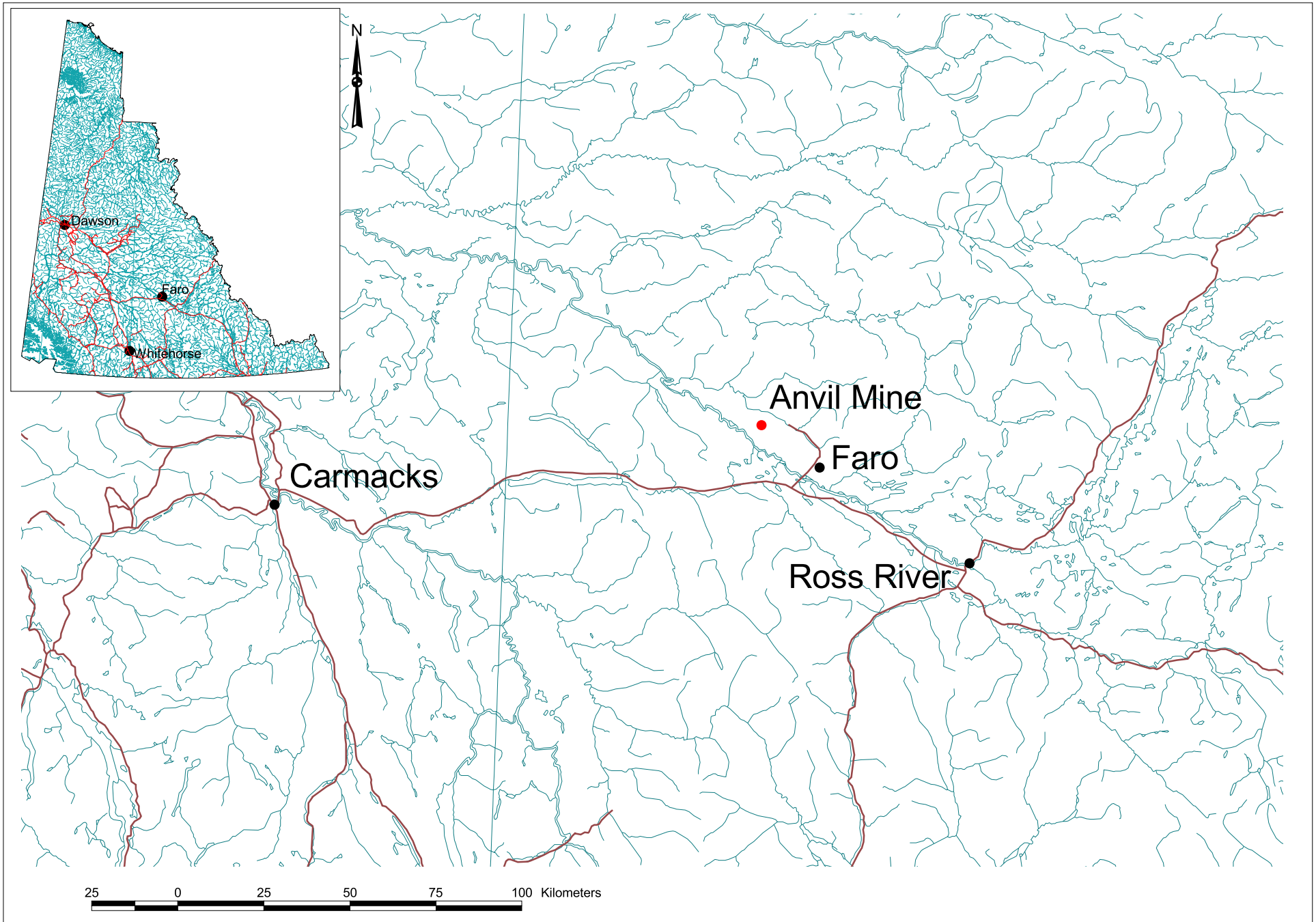


Figure 2 - Regional Geology

